Tuning the Binding Dynamics of a Guest-Octaacid Capsule through Noncovalent Anchoring

Suma S. Thomas, Hao Tang, Adam Gaudes, Signe B. Baggesen, Corinne L. D. Gibb, Bruce C. Gibb, & Cornelia Bohne

May 2017

Tuning the Binding Dynamics of a Guest-Octaacid Capsule through Non-Covalent Anchoring

Suma S. Thomas[†] *Hao Tang*[†,&] *Adam Gaudes*[†] *Signe B. Baggesen*[†] *Corrine L. D. Gibb*[‡] *Bruce C. Gibb,**[,‡] *and Cornelia Bohne**[,†]

[†], Department of Chemistry, University of Victoria, PO Box 1700 STN CSC, Victoria, BC, Canada V8W 2Y2

[‡], Department of Chemistry, Tulane University, New Orleans, Louisiana 70118, United States

[&], current position: School of Chemistry and Chemical Engineering, South China University of Technology, 381 Wushan Road, Guangzhou 510641, China

Corresponding authors: cornelia.bohne@gmail.com; bgibb@tulane.edu

Abstract. Hydrophobic or hydrophilic substituents have different effects on the binding dynamics of pyrene derivatives with a 2:1 capsule formed from two octaacid cavitands, showing a subtle interplay of different kinetic factors. Anchoring of the methyl group of 1-methylpyrene within one cavitand slowed the association and dissociation dynamics of the 1:1 complex by at least 1,000 times when compared to the 1:1 complex for pyrene. This slow down for the transient formation of the 1:1 complex is responsible for the overall increase in stability of the 2:1 complex without affecting the overall capsule dissociation. For 1-pyrenemethanol, its residence time in the 2:1 capsule is shorter compared to pyrene despite both guests having similar equilibrium constants for the binding of the second cavitand, suggesting that the hydroxymethyl substituent close to the equatorial region of the capsule can interact with water during the partial opening of the capsule.

TOC GRAPHIC

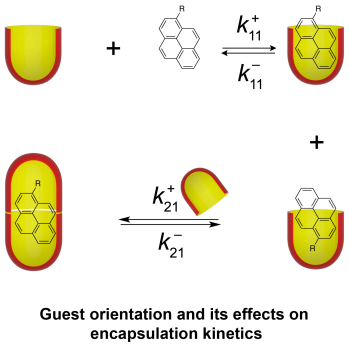

Guest orientation and its effects on encapsulation kinetics

Container molecules provide the ability to control chemistry in constraint environments. Self-assembled containers with the ability for controlled cargo release are of importance for functional materials targeted for separations, catalysis, transport or drug delivery.[1-4] The self-assembled octaacid cavitand (OA, Chart 1)[5] has been used to alter the reactivity of complexed guests,[5-8] achieve the physical separation of gases,[9] and recognition of alkane and halo-alkane isomers[10], as well as the kinetic resolution of constitutional isomeric esters.[11] In such cases the structure of the guest dictates the number of guests encapsulated[5] and their packing affects the outcome of reactions within the capsule.[7] Spatial restrictions and guest-capsule interactions influence the mobility of the guest, where rotation along the long axis of the guest can occur in nanoseconds,[12] while the partial opening at the equatorial region of the capsule (so-called capsule "breathing") which enables the entry of small molecules like oxygen, occurs in the microsecond timescale.[13-14] In contrast, complete dissociation of the capsule with release of the guest is much slower, which in the case of pyrene (Py) occurred in 2.7 s.[15] Controlling guest dissociation is of relevance for applications where the release from the capsule is related to the observed reactivity, as was the case for the kinetic resolution of esters,[11] or where release of a product is desired, such as for the photorelease of water soluble products from hydrophobic precursors.[16-19] Furthermore, singlet oxygen reactivity has provided indirect evidence that the capsule opening time is dependent on the structure of the guest.[13] The objective of the present study was to determine how hydrophobic and hydrophilic substituents affect the OA-guest capsule dynamics and how these changes are related to the overall stability of the capsule; to accomplish this we used stopped-flow fluorescence experiments to circumnavigate the issue that kinetic pathways cannot be inferred from the determination of equilibrium constants.[20]

Chart 1. Chemical structures of octaacid (OA), pyrene (Py), 1-pyrenemethanol (PyMeOH) and 1-methylpyrene (MePy).

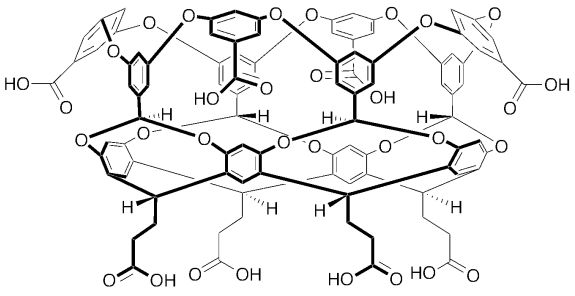

OA

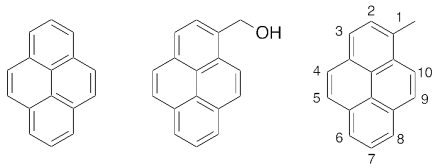

Py PyMeOH MePy

A combination of optimal filling and attractive interactions between host and guest result in the terminal moiety of chains, or protuberances on a ring of the guest, locating into the narrow, base region of the cavitand.[21-27] Consequently, these terminal groups or protuberances can act as anchors and control guest orientation within the capsule. Based on this idea, we chose 1-methylpyrene (MePy) and 1-pyrenemethanol (PyMeOH) (chart 1) as guests to probe how guest orientation influences the capsule assembly kinetics. These guests are of lower symmetry than Py and can form two different 1:1 complexes with different orientations for the guests with respect to the host (Scheme 1, $(G:OA)_{in}$ and $(G:OA)_{out}$). As we show, anchoring of the hydrophobic methyl group in the base region slowed the dynamics of $(MePy:OA)_{in}$ by at least 1,000 times compared to the formation of the 1:1 complex for Py, while the hydroxymethyl substituent did not significantly affect the binding dynamics for the 1:1 complex. The slow down for the transient formation of $(MePy:OA)_{in}$ translates into the higher stability of the OA:MePy:OA capsule without significantly affecting the overall capsule dissociation, providing an example of the uncoupling between the kinetics and thermodynamics of a host-guest system.

Scheme 1. Formation of orientational isomeric 1:1 complexes between OA and formation of the corresponding 2:1 capsule.

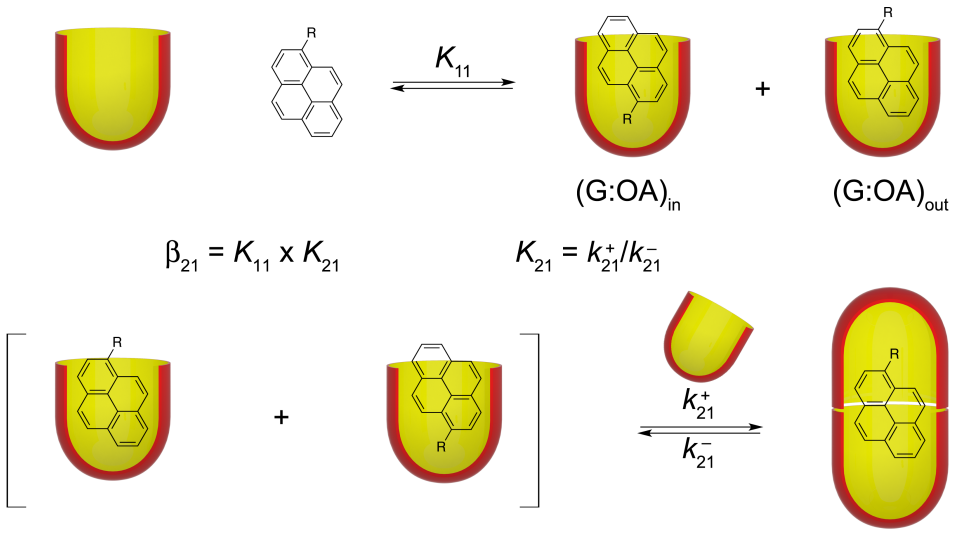

Binding isotherms were determined from changes in the intensities of emission or excitation fluorescence spectra (see the Supporting Information for experimental details) based on similar changes observed for Py (K_{11} = (4.5 ± 0.6) × 10^5 M^{-1}, K_{21} = (7 ± 1) × 10^6 M^{-1}).[15] For PyMeOH, isoemissive points were observed for some of excitation and emission spectra, but not all (Fig. 1a, Fig. S1 in the Supporting Information), suggesting the presence of more than two emissive species corresponding to free PyMeOH and different OA complexes. The binding isotherm could not be fit to a sequential model (Fig. S2, see the Supporting Information for all models used for the fits of binding isotherms and kinetics), suggesting that the individual complexes could not be resolved. The overall equilibrium constant, β_{21}, for OA:PyMeOH:OA (Fig. 1b) of (1.18 ± 0.04) × 10^{12} M^{-2} is lower compared to the value for Py ((3.19 ± 0.06) × 10^{12} M^{-2}),[15] suggesting that the presence of the hydroxymethyl group destabilizes the capsule. The K_{11} value for PyMeOH of (1.2 ± 0.3) × 10^5 M^{-1} was determined from kinetic studies (see below) and when this value was fixed for the fit of the binding isotherm a value of (1.4 ± 0.2) × 10^7 M^{-1} was

recovered for K_{21} which led to a calculated overall binding constant ($\beta_{21} = K_{11} \times K_{21}$) of (1.7 ± 0.3) × 10^{12} M^{-2} consistent with the β_1 value obtained from the overall binding model.

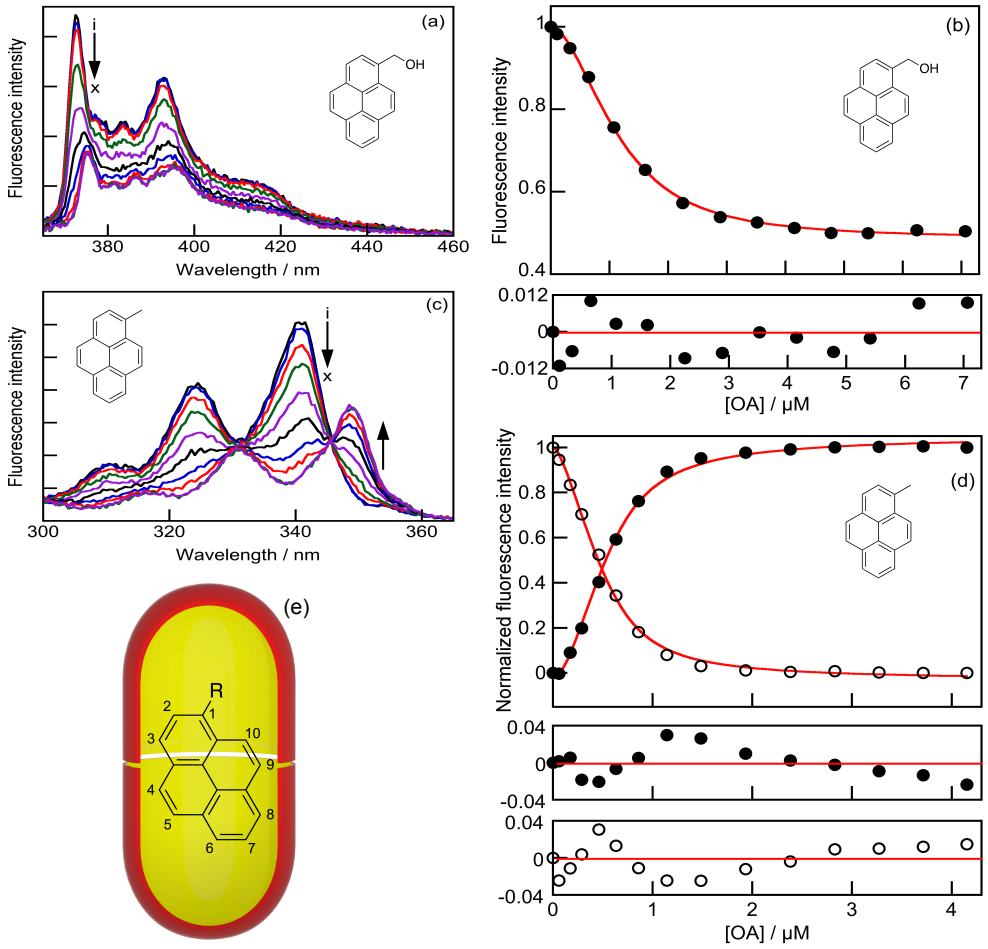

Figure 1. (a) Fluorescence emission spectra (λ_{ex} = 340 nm) for 0.2 μM PyMeOH in the absence (i, black) and presence of up to 7.1 μM OA (ii to x). (b) Fit and the corresponding residuals for the dependence of emission intensity on OA concentration for 0.2 μM PyMeOH to an overall 2:1 complex binding model. (c) Fluorescence excitation spectra (λ_{em} = 374 nm) for 0.2 μM MePy in the absence (i, black) and presence of up to 4.2 μM OA (ii to x). (d) Fits and the corresponding residuals for the dependence of integrated intensities on OA concentration for 0.2 μM MePy to a sequential binding model where the increasing (peak at 349 nm) and decreasing (peak at 340 nm) intensities of the excitation spectra were fit simultaneously using global analysis. The amplitudes for binding isotherms are normalized. (e) Orientation of MePy inside OA capsule derived from ^{1}H NMR studies.

The presence of isoemissive points when MePy was bound to OA was also dependent on the excitation and emission wavelengths (Fig. S3 in the Supporting Information), but in contrast to PyMeOH the binding isotherm fit with a sequential model (Fig. 1c, d, Fig. S4 in the Supporting Information) yielding K_{11} and K_{21} values of $(1.6 \pm 0.5) \times 10^6$ M^{-1} and $(1.4 \pm 0.1) \times 10^7$ M^{-1}. The calculated β_{21} value of $(2.2 \pm 0.7) \times 10^{13}$ M^{-2} for OA:MePy:OA shows that binding of this guest is stronger than the binding of Py or PyMeOH to the capsule.

The orientation of MePy in the OA capsule was studied using ^{1}H NMR, where all guest signals were identified by a combination of COSY and NOESY (Figs. S5, S6 in the Supporting Information). Calculation of the difference between the ^{1}H NMR peak positions of the guest in the free (1:1 D_2O-DMSO-d_6) and the bound state ($\Delta\delta$) prove useful because the truncated cone shape of the pocket means that, to a first approximation, the deeper the position of an atom of the guest inside the pocket, the greater its upfield shift.[28] However, NMR revealed no evidence for the presence of the 1:1 complex. For the 2:1 complex, it was found that the signals from the 6-, 7-, and 8-positions (Fig. 1e) were the most upfield shifted ($\Delta\delta$ = -4.01, -3.24 and -2.67 respectively), followed by the signals for the 1-Me and 2-position ($\Delta\delta$ = -2.55 and -2.76 respectively), and then the signals corresponding to the H-atoms at positions 4- and 9- ($\Delta\delta$ = -0.74 and -1.33 respectively). The overall peak shifts suggest a preferred binding orientation within the nano-space in which the 6-, 7- and 8- protons are most deeply located in the cavity of one host, the protons on the methyl, 2- and 3- positions less so in the other "hemisphere", and the H-atoms at positions 4- and 9- located in the equatorial region (Fig. 1e).

The kinetics of systems with multiple species leads to several relaxation processes.[20] The dynamics of the 1:1 Py:OA complex is faster than the 1 ms time resolution of the stopped-flow

experiment leading to an immediate off-set in intensity when the solutions of Py and OA are mixed.[15] The K_{11} value (Table 1) was determined from the binding isotherm constructed from these off-sets. The off-set is followed by first-order kinetics for the formation of the 2:1 capsule. The association rate constant (k_{21}^{+}) was determined from the global analysis of the kinetics at varying OA concentrations, while the dissociation rate constant (k_{21}^{-}) was calculated from the values of k_{21}^{+} and K_{21}.[15] The binding kinetics of PyMeOH with OA also showed an intensity off-set followed by first-order kinetics (Fig. 2a, Fig. S7 in the Supporting Information), suggesting that two relaxation processes occurred. The K_{11} value of $(1.2 \pm 0.3) \times 10^5$ M^{-1} (Table 1) determined from the binding isotherm (Fig. 2b) was used to calculate a K_{21} value of $(1.0 \pm 0.3) \times 10^7$ M^{-1} from the β_{21} value ($(1.18 \pm 0.04) \times 10^{12}$ M^{-2}) (Table 1). The kinetics after the off-set were fit using global analysis to a model where a fast equilibrium is followed by capsule formation (Fig. 2c, d). The K_{11} values were fixed between the limits determined by the error of this parameter leading to k_{21}^{+} and k_{21}^{-} values that were averaged (Table S1 in the Supporting Information). The averages from two independent experiments for k_{21}^{+} and k_{21}^{-} are $(7 \pm 2) \times 10^6$ M^{-1} s^{-1} and (0.7 ± 0.1) s^{-1}. The value for K_{21} calculated from the ratio of these rate constants ($(1.0 \pm 0.3) \times 10^7$ M^{-1}) is the same as the one obtained from the analysis of the binding isotherm (Table 1). The analysis for the kinetics of OA:PyMeOH:OA formation differed from the analysis for the binding with Py because of the explicit inclusion of k_{21}^{-} in the model. Analysis of the PyMeOH kinetics using the previous method[15] (Scheme S1 and Table S2 in the Supporting Information) led to the same rate constants ensuring that the differences in these values for Py and PyMeOH were not because we used different models.

Table 1. Equilibrium constants and association and dissociation rate constants for the binding of Py, PyMeOH and MePy with the OA cavitand in a 1:1 complex and with the OA capsule (2:1 complex).

parameters	**Py**[a]	**PyMeOH**	**MePy**
β_{21} / 10^{12} M^{-2}	3.19 ± 0.06	1.18 ± 0.04	22 ± 7[b]
K_{11} / 10^{5} M^{-1}	4.5 ± 0.6	1.2 ± 0.3[c]	16 ± 5
K_{21} / 10^{6} M^{-1}	7 ± 1	10 ± 3[d]	14 ± 1
k_{21}^{+} / 10^{6} M^{-1} s^{-1}	2.6 ± 0.2	7 ± 2	0.153 ± 0.002[e]
			6.8 ± 0.1[f]
k_{21}^{-} / s^{-1}	0.37 ± 0.06	0.7 ± 0.1	-
τ_{dis} / s[g]	2.7 ± 0.4	1.4 ± 0.2	-

[a], from reference 14;[15] [b], calculated from K_{11} and K_{21} values; [c], obtained from kinetic studies; [d], calculated from K_{11} and β_{21}; [e], value for the reaction of $(MePy:OA)_{in}$; [f], value for the reaction of $(MePy:OA)_{out}$; [g], $1/k_{21}^{-}$.

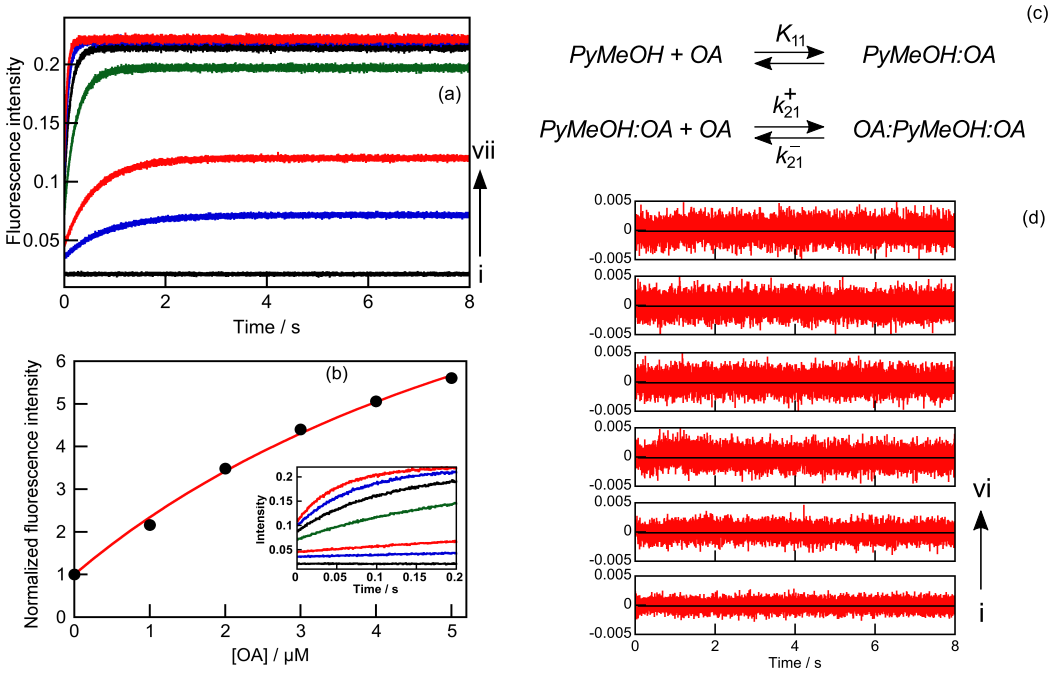

Figure 2. Binding of PyMeOH with OA: (a) Mixing of a PyMeOH solution (0.2 μM) with a solution in the absence (i-black) and presence of OA (0.7, ii-blue; 1.0 iii-red; 2.0, iv-green; 3.0, v-black; 4.0, vi-blue and 5 μM, vii-red). All concentrations are final ones after mixing. (b) Binding isotherm fit to a 1:1 complex binding model obtained from the offsets for the initial intensities (inset) for the stopped-flow experiment. (c) Model used in the global analysis of kinetic traces. (d) Residuals obtained for the global analysis using the model in (c) for the data in (a). From bottom (i) to top (vi) panel the concentration of OA increases from 0.7 to 5 μM.

The K_{11} value for PyMeOH is smaller by a factor of 3.8 when compared to Py. K_{11} corresponds to the sum of the equilibrium constants for the formation of $(PyMeOH:OA)_{in}$ and $(PyMeOH:OA)_{out}$. Based on previous precedent, which showed that hydrophilic moieties are located at the opening of OA,[22, 29] and the fact that one relaxation process follows the formation of the 1:1 complex, $(PyMeOH:OA)_{out}$ is likely the predominant 1:1 complex formed. In this case, the value for K_{11} is expected to be lower by a factor of two,[30] since only one extremity binds to the OA cavitand, while for Py both extremities can bind. This prediction is in line with the lower K_{11} value observed for PyMeOH. The higher k_{21}^{+} and k_{21}^{-} values for PyMeOH compared to Py indicate that the dynamics for the capsule containing PyMeOH is faster than for Py, resulting in a shorter

residence time for PyMeOH (1.4 s) than for Py (2.7 s) probably because during the many "breathing" motions of the capsule water has access to the guest and solvates the alcohol moiety leading to the break up of the capsule. However, since both the association and dissociation processes are faster for PyMeOH, the similar K_{21} values for PyMeOH and Py stress that the value of this equilibrium constant is not a good predictor of the residence time of the guest in the capsule.

The kinetics for the binding of MePy with OA (Fig. 3a) shows a smaller off-set than measured for Py or PyMeOH followed by kinetics that could not be fit to a mono-exponential function. The kinetics were adequately fit to the sum of two exponentials indicating that binding of MePy to OA has three relaxation processes, where one process is fast and two processes are slow. The kinetics fit well using global analysis (Fig. 3c) to a model (Fig. 3b) where one 1:1 complex is formed in fast equilibrium followed by the formation of the second 1:1 complex and the 2:1 capsule (see the Supporting Information for possible models considered that are not consistent with the data). The fast equilibrium was assigned to the formation of $(MePy:OA)_{out}$ in analogy to the inclusion of Py. The small amplitude observed for the off-set precluded the determination of K_{11}^{out} (Fig. S8 in the Supporting Information). This small amplitude is consistent with the formation of only one of the 1:1 complexes during the mixing time of the stopped-flow experiment. If the formation of both 1:1 complexes occurred during the mixing time then a higher intensity would be expected for the off-set based on the changes seen for the fluorescence binding studies.

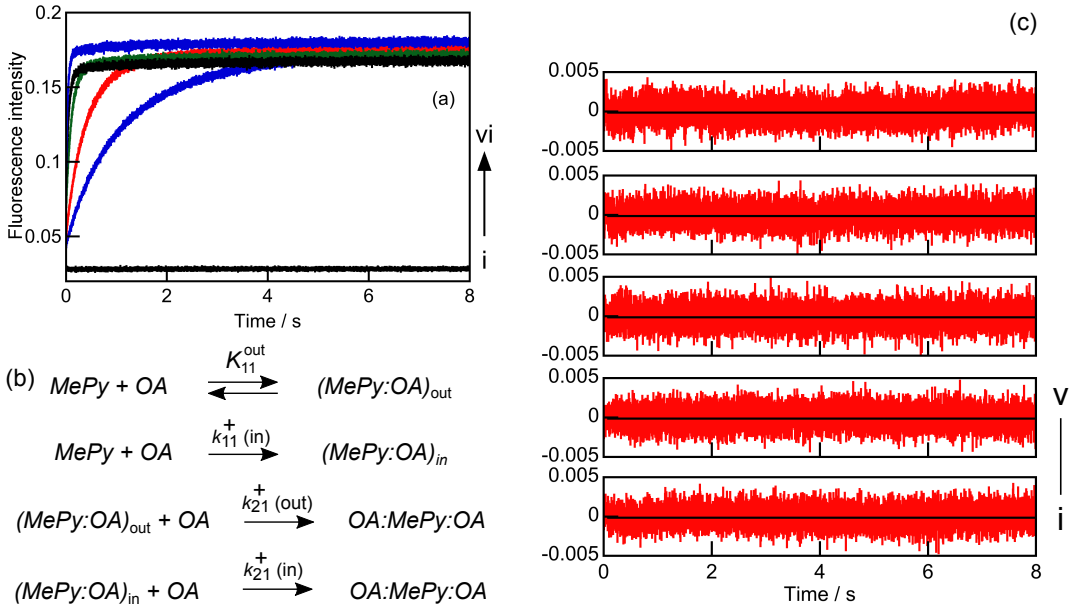

Figure 3. Binding of MePy with OA: (a) Mixing a MePy solution (0.2 μM) with a solution in the absence (i-black) and presence of OA (1.0, ii-blue; 2.0, iii-red; 3.0, iv-green; 4.0, v-black and 5.0 μM, vi-blue) at OA concentrations close to the saturation of the binding isotherm (Fig. 1d). All concentrations are final ones after mixing. (b) Model used for the analysis of the kinetics. (c) Residuals obtained for the global analysis using the model in (b) for the data in (a). From bottom (i) to top (v) panel the concentration of OA increases from 1.0 to 5.0 μM.

The two relaxation processes following the initial off-set correspond to the formation of the $(MePy:OA)_{in}$ 1:1 complex and the 2:1 capsule in processes that are coupled. This fact precludes the assignment of the individual relaxation processes to the formation of individual complexes. The model that adequately fits the data (Fig. 3b, c; see the Supporting Information for other models that did not fit; Fig. S9, S10; Scheme S2, S3, S4) includes the fast and slow formation of the two 1:1 complexes and the formation of the capsule from both 1:1 complexes. Inclusion of dissociation rate constants into the model did not lead to the recovery of these parameters because they were too low. Formation of the capsule only from the most stable $(MePy:OA)_{in}$ complex led to inadequate fits. The value for K_{11}^{out} was fixed in the fit to the value determined for PyMeOH (1.2×10^5 M^{-1}), which corresponds to the lower limit for this parameter. Fixing

K_{11}^{out} to the higher limit defined by the K_{11} value for Py led to inconsistent association rate constants. The association rate constant for $(MePy:OA)_{in}$ formation (k_{11}^{+}) varied between 2×10^5 and 8×10^5 M^{-1} s^{-1} for two independent experiments. This variability reflects the small contribution of the formation of $(MePy:OA)_{in}$ to the amplitude of the overall kinetics. The range from 0.1 to 0.7 s^{-1} was calculated for the dissociation rate constant of $(MePy:OA)_{in}$ from K_{11}^{in} ($1.6 \pm 0.5) \times 10^6$ M^{-1} and the range of k_{11}^{+} values. The dynamics for $(MePy:OA)_{in}$ formation is slowed by at least 1,000 times compared to Py:OA and k_{11}^{+} is lower than the association rate constant of the second OA in the case of Py:OA. This result shows that the nesting of the methyl group in the OA cavitand requires a higher activation free energy than for the incorporation of Py. However once formed, $(MePy:OA)_{in}$ is more stable than the 1:1 complexes with Py and PyMeOH leading to a residence time of MePy in the $(MePy:OA)_{in}$ 1:1 complex that is of the same order of magnitude as for the 2:1 capsules containing Py or PyMeOH.

The association rate constant of the second OA to $(MePy:OA)_{in}$ is lower than for $(MePy:OA)_{out}$ suggesting that the positioning of the methyl group inside the OA cavitand for $(MePy:OA)_{in}$ rigidifies the complex slowing the binding of the second OA. This slow down is likely due to required distortions of the cavitand or introduction of repulsive interactions to achieve the capping of the $(MePy:OA)_{in}$ 1:1 complex by the second OA. The slow capsule formation from $(MePy:OA)_{in}$ makes possible the transient observation of $(MePy:OA)_{in}$. Further analysis of the dynamics for capsule formation is hampered by the unavailability of the individual dissociation rate constants of the 2:1 capsule to form each of the 1:1 complexes.

The slow down of the binding dynamics for $(MePy:OA)_{in}$ is reflected in the higher K_{11} value for this complex suggesting that it might be detectable at low OA concentrations (Fig. S11 in the

Supporting Information). Differentiation of fluorescent species in different environments is possible with time-resolved experiments when excited-state quenchers have different access to the fluorophores in the different environments.[20] Quenching of PyMeOH by nitromethane, a known quencher for Py,[31] in the presence of OA showed that the quenching rate constant for the capsule was 500 times lower than for PyMeOH in water (Figs. S12, S13 and Table S3 in the Supporting Information). In the case of MePy three species were observed where one species had an intermediate quenching efficiency between that for MePy in water and in the capsule, showing that $(MePy:OA)_{in}$ was observable as predicted from the kinetic complex formation studies (Figs. S14, S15 and Table S4 in the Supporting Information).

Our findings are relevant to the development of tools in the area of systems chemistry,[32-35] where the ultimate objective is to build up and control the emergent properties of a system, *de novo*. As described here, the introduction of substituents on Py lowers its symmetry and increases the complexity for the speciation in the host-guest system from three (free Py, 1:1 and 2:1 complexes), to four (free guest, two 1:1 complexes and 2:1 complex). The effects of this are not directly observable from thermodynamic analyses. Thus the formation of the $(MePy:OA)_{in}$ is relatively slow, and the association and dissociation dynamics for the formation of the 2:1 PyMeOH complex from the corresponding 1:1 complex are relatively fast, but neither are evident from the overall equilibrium constants for all three complexes discussed here. These results underscore the power of structure-dynamics relationship studies to further the understanding of how systems chemistry and complexity can be controlled.

ACKNOWLEDGMENT

The authors at UVic thank the Natural Sciences and Engineering Research Council of Canada (NSERC) for financial support (RGPIN-121389-2012). BCG and CLDG gratefully acknowledge the support of the National Institutes of Health (GM 098141).

ASSOCIATED CONTENT

Supporting Information. Available free of charge containing: Experimental section, model for fitting binding isotherms, excitation and emission spectra, NMR analysis, kinetic analysis and quenching experiments.

AUTHOR INFORMATION

ORCID

Cornelia Bohne: orcid.org/0000-0001-9996-0076

Bruce Gibb: orcid.org/0000-0002-4478-4084

Suma S. Thomas: orcid.org/0000-0001-5514-4288

Hao Tang: orcid.org/0000-0003-1063-881X

Notes

The authors declare no competing financial interests.

REFERENCES

1. Hooley, R. J.; Rebek Jr, J. Chemistry and Catalysis in Functional Cavitands. *Chem. Biol.* ***2009***, 16, 255-264.
2. Liu, F.; Wang, H.; Houk, K. N. Gating in Host-Guest Chemistry. *Curr. Org. Chem.* ***2013***, 17, 1470-1480.
3. Ma, X.; Zhao, Y. Biomedical Applications of Supramolecular Systems Based on Host–Guest Interactions. *Chem. Rev.* ***2015***, 115, 7794-7839.
4. Rudkevich, D. M. Progress in Supramolecular Chemistry of Gases. *Eur. J.Org. Chem.* ***2007***, 2007, 3255-3270.

5. Jordan, J. H.; Gibb, B. C. Molecular Containers Assembled through the Hydrophobic Effect. *Chem. Soc. Rev.* ***2015***, 44, 547-585.
6. Ramamurthy, V. Photochemistry within a Water-Soluble Organic Capsule. *Acc. Chem. Res.* ***2015***, 48, 2904-2917.
7. Ramamurthy, V.; Jokusch, S.; Porel, M. Supramolecular Photochemistry in Solution and on Surfaces: Encapsulation and Dynamics of Guest Molecules and Communication between Encapsulated and Free Molecules. *Langmuir* ***2015***, 31, 5554-5570.
8. Ramamurthy, V.; Sivaguru, J. Supramolecular Photochemistry as a Potential Synthetic Tool: Photocycloaddition. *Chem. Rev.* ***2016***, 116, 9914-9993.
9. Gibb, C. L. D.; Gibb, B. C. Templated Assembly of Water-Soluble Nano-Capsules: Inter-Phase Sequestration, Storage, and Separation of Hydrocarbon Gases. *J. Am. Chem. Soc.* ***2006***, 128, 16498-16499.
10. Sullivan, M. R.; Gibb, B. C. Differentiation of Small Alkane and Alkyl Halide Constitutional Isomers Via Encapsulation. *Org. Biomol. Chem.* ***2015***, 13, 1869-1877.
11. Liu, S.; Gan, H.; Hermann, A. T.; Rick, S. W.; Gibb, B. C. Kinetic Resolution of Constitutional Isomers Controlled by Selective Protection inside a Supramolecular Nanocapsule. *Nat. Chem.* ***2010***, 2, 847-852.
12. Kulasekharan, R.; Jayaraj, N.; Porel, M.; Choudhury, R.; Sundaresan, A. K.; Parthasarathy, A.; Ottaviani, M. F.; Jokusch, S.; Turro, N. J.; Ramamurthy, V. Guest Rotations within a Capsuleplex Probed by NMR and EPR Techniques. *Langmuir* ***2010***, 26, 6943-6953.
13. Natarajan, A.; Kaanumalle, L. S.; Jockusch, S.; Gibb, C. L. D.; Gibb, B. C.; Turro, N. J.; Ramamurthy, V. Controlling Photoreactions with Restricted Spaces and Weak Intermolecular Forces: Exquisite Selectivity During Oxidation of Olefins by Singlet Oxygen. *J. Am. Chem. Soc.* ***2007***, 129, 4132-4133.
14. Jayaraj, N.; Jokusch, S.; Kaanumalle, L.; Turro, N. J.; Ramamurthy, V. Dynamics of Capsuleplex Formed between Octaacid and Organic Guest Molecules — Photophysical Techniques Reveal the Opening and Closing of Capsuleplex. *Can. J. Chem.* ***2011***, 89, 203-213.
15. Tang, H.; de Oliveira, C. S.; Sonntag, G.; Gibb, C. L. D.; Gibb, B. C.; Bohne, C. Dynamics of a Supramolecular Capsule Assembly with Pyrene. *J. Am. Chem Soc.* ***2012***, 134, 5544-5547.
16. Raj, A. M.; Raymo, F. M.; Ramamurthy, V. Reversible Disassembly–Assembly of Octa Acid–Guest Capsule in Water Triggered by a Photochromic Process. *Org. Lett.* ***2016***, 18, 1566-1569.
17. Kamathan, N.; Mendes, D. C.; da Silva, J. P.; Givens, R. S.; Ramamurthy, V. Photorelease of Incarcerated Caged Acids from Hydrophobic Coumaryl Esters into Aqueous Solution. *Org Lett.* ***2016***, 18, 5480-5483.
18. Jagadesan, P.; da Silva, J. P.; Givens, R. S.; Ramamurthy, V. Photorelease of Incarcerated Guests in Aqueous Solution with Phenacyl Esters as the Trigger. *Org. Lett.* ***2015***, 17, 1276-1279.
19. Jayaraj, N.; Jagadesan, P.; Samanta, S. R.; da Silva, J. P.; Ramamurthy, V. Release of Guests from Encapsulated Masked Hydrophobic Precursors by a Phototrigger. *Org. Let.* ***2013***, 15, 4374-4377.
20. Bohne, C. Supramolecular Dynamics. *Chem. Soc. Rev.* ***2014***, 43, 4037-4050.
21. Gibb, C. L. D.; Gibb, B. C. Straight-Chain Alkanes Template the Assembly of Water-Soluble Nano-Capsules. *Chem. Commun.* ***2007***, 1635-1637.

22. Sun, H.; Gibb, C. L. D.; Gibb, B. C. Calorimetric Analysis of the 1:1 Complexes Formed between a Water-Soluble Deep-Cavity Cavitand, and Cyclic and Acyclic Carboxylic Acids. *Supramol. Chem.* ***2008***, 20, 141-147.
23. Gibb, C. L. D.; Gibb, B. C. Guests of Differing Polarities Provide Insight into Structural Requirements for Templates of Water-Soluble Nano-Capsules. *Tetrahedron* ***2009***, 65, 7240-7248.
24. Jayaraj, N.; Zhao, Y.; Parthasarathy, A.; Porel, M.; Liu, R. S. H.; Ramamurthy, V. Nature of Supramolecular Complexes Controlled by the Structure of the Guest Molecules: Formation of Octa Acid Based Capsuleplex and Cavitandplex. *Langmuir* ***2009***, 25, 10575-10586.
25. Porel, M.; Jayaraj, N.; Kaanumalle, L. S.; Maddipatla, M. V. S. N.; Parthasarathy, A.; Ramamurthy, V. Cavitand Octa Acid Forms a Nonpolar Capsuleplex Dependent on the Molecular Size and Hydrophobicity of the Guest. *Langmuir* ***2009***, 25, 3473-3481.
26. Choudhurym, R.; Barman, A.; Prabhakar, R.; Ramamurthy, V. Hydrocarbons Depending on the Chain Length and Head Group Adopt Different Conformations within a Water-Soluble Nanocapsule: 1H NMR and Molecular Dynamics Studies. *J. Phys. Chem. B* ***2013***, 117, 398-407.
27. Gibb, C. L. D.; Gibb, B. C. Binding of Cyclic Carboxylates to Octa-Acid Deep-Cavity Cavitand. *J. Comput. Aided Mol. Des.* ***2014***, 28, 319-325.
28. Barnett, J. W.; Gibb, B. C.; Henry S. Ashbaugh, H. S. Succession of Alkane Conformational Motifs Bound within Hydrophobic Supramolecular Capsular Assemblies. *J. Phys. Chem. B* ***2016***, 120, 10394-10402.
29. Sullivan, M. R.; Sokkalingam, P.; Nguyen, T.; Donahue, J. P.; Gibb, B. C. Binding of Carboxylate and Trimethylammonium Salts to Octa-Acid and Temoa Deep-Cavity Cavitands. *J. Comput. Aided Mol. Des.* ***2017***, 31, 21-28.
30. Connors, K. A., *Binding Constants - the Measurement of Molecular Complex Stability*; John Wiley & Sons: New York, 1987.
31. Chen, M.; Grätzel, M.; Thomas, J. K. Kinetic Studies in Bile Acid Micelles. *J. Am. Chem. Soc.* ***1975***, 97, 2052-2057.
32. Ludlow, R. F.; Otto, S. Systems Chemistry. *Chem. Soc. Rev.* ***2008***, 37, 101-108.
33. Ashkenasy, G.; Hermans, T. M.; Otto, S.; Taylor, A. F. Systems Chemistry. *Chem. Soc. Rev.* ***2017***, 46, 2543-2554.
34. von Kiedrowski, G.; Otto, S.; Herdewijn, P. Welcome Home, Systems Chemists! *J. Syst. Chem.* ***2010***, 1:1, 1-6.
35. Showalter, K.; Epstein, I. R. From Chemical Systems to Systems Chemistry: Patterns in Space and Time. *Chaos* ***2015***, 25, 097613/097611-097613.